energies

Article

Arc-Extinguishing Research on Semi-Closed Multi-Compression Tube Structures

Yongfeng Song *, Jufeng Wang, Ping Huang, Yang Lu, Qiwen He, Zhenghao Jia, Hao Li and Yanlei Wang

High-Voltage Laboratory, Guangxi University, Nanning 530004, China
* Correspondence: cvx730425@outlook.com

Abstract: Using lightning energy to extinguish the arc is a new lightning protection method. On this basis, the semi-closed multi-compression tube structures (SMTS) combined with the arc extinguishing structure studied in this paper can suppress the power frequency arc at the initial stage of arc establishment by using the coupling effect of current and gas. Firstly, through the simulation comparison method, the promotion effect of the semi-closed tube on the arc discharge was found. Furthermore, the two-dimensional impulse power frequency current coupling discharge model was established to obtain changes in physical quantities, such as temperature and conductivity. The conductivity decreased to the initial value in about 1 ms. Finally, the impulse power frequency combined arc extinguishing test was carried out. The test results show that the arc extinguishing structure can effectively extinguish power frequency freewheeling within 1 ms. It proves the effectiveness of the arc extinguishing structure.

Keywords: arc quenching; impulse arc; power frequency freewheeling; magnetohydrodynamics

1. Introduction

Lightning overvoltage severely threatens the safe operation of power grid lines. In some areas with high occurrences of lightning accidents, most overhead lines are easily damaged by lightning strikes [1–4], and they cause about 70% of tripping accidents. When a lightning strike occurs, the power frequency arc generated at the insulator is the leading cause of short-circuit fault and line tripping. Therefore, how to quickly discharge the lightning energy, cut off the short-circuit path, and restore the dielectric insulation has become a hot and challenging research topic for scholars in recent years [5,6]. The gas arc extinguishing and lightning protection method is a new lightning protection method developed in recent years. Protecting lightning strike conditions, such as counterattacks in the soil resistivity area, can eliminate the constraints of uncontrollable factors, such as ground grid resistance, lightning strike intensity, and shielding [7–9] .

Gas arc-extinguishing lightning protection methods are divided into active arc extinguishing and self-energy arc extinguishing [10–15]. Active arc extinguishing mainly uses gas blowing to extinguish the arc. When the arc passes through the chamber of the arc-extinguishing device, the lightning pulse generated by the lightning strike triggers the gas-generating material, releases high-temperature and high-pressure gas, and accelerates the deionization process of the arc. However, the continuous arc-extinguishing ability is limited due to the limited number of arc extinguishers. The self-energy arc-extinguishing method used in this paper can generate arc-extinguishing gas by utilizing the coupling effect between the arc's energy and the air's energy. This method can divide the long-gap arc into short arcs and confine them in multiple semi-sealed chambers, which has a long-lasting arc-extinguishing ability.

This paper proposes a combined arc-extinguishing structure using semi-closed multi-compression tubes suitable for 10–35 kV distribution lines. When the arc enters the multi-compression tube from outer space, it uses its energy conversion and contacts the cold wall

check for updates

Citation: Song, Y.; Wang, J.; Huang, P.; Lu, Y.; He, Q.; Jia, Z.; Li, H.; Wang, Y. Arc-Extinguishing Research on Semi-Closed Multi-Compression Tube Structures. *Energies* **2023**, *16*, 1057. https://doi.org/10.3390/en16031057

Academic Editor: Andrea Mariscotti

Received: 30 November 2022
Revised: 5 January 2023
Accepted: 16 January 2023
Published: 18 January 2023

of the tube to form a high-speed airflow. Based on the principle of high-speed airflow, a two-dimensional arc-extinguishing model of SMTS was built through the Comsol Multiphysics simulation software. The function of SMTS during arc extinguishing is analyzed, and the reliability of SMTS is proved by the impact power frequency combined arc extinguishing test and the actual operation effect.

2. Components and Arc-Extinguishing Principle of SMTS

2.1. Components

Figure 1a shows the appearance of semi-closed multi-compression tube structures (SMTS), which consist of semi-closed tubes, multiple arc-extinguishing tubes, metal electrodes, skirts, insulating surfaces, and ground electrodes. The arc-extinguishing tubes are arranged in a zigzag shape to form multiple arc-extinguishing tubes. Each arc-extinguishing tube includes an arc-extinguishing tube wall, an arc-extinguishing channel, and a metal electrode.

The semi-closed structure uses the expansion of the arc channel to generate shock waves to squeeze the air layer to form reflected waves, which weakens the development process of the arc; the multi-pipe structure can constrain the arc path. With the effect of compression and current transient heat conduction, the arc temperature rises rapidly, and the gas is heated to cause the pressure to increase, forming a high-speed airflow that is removed along the fracture, blocking the continuity of the arc energy.

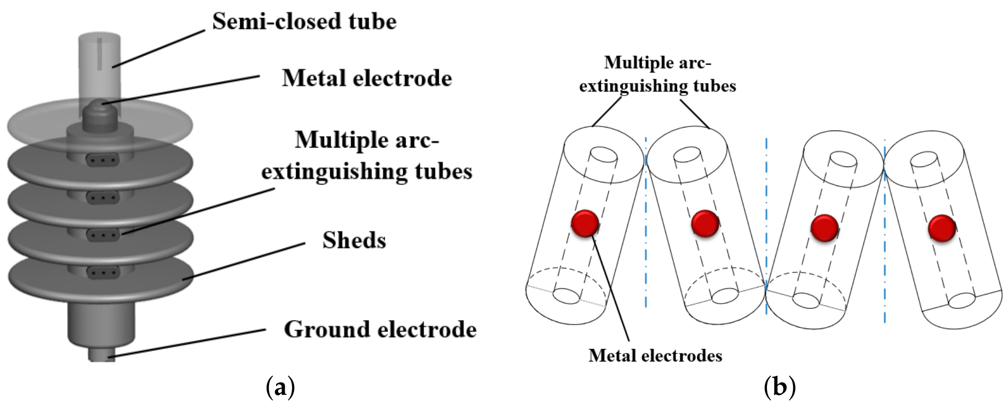

Figure 1. Structural schematic diagram of semi-closed multi-compression tube structures (SMTS): (**a**) The appearance of SMTS. (**b**) The internal structure of the multi-compression tubes.

2.2. Arc-Extinguishing Principle

The arc entry into the semi-closed compression tube is the arc discharge process in a narrow and long space, thus assuming that the entire arc is at the same temperature at the same instant [16]. According to the heat balance relationship, the decrease in the internal energy of the arc is equal to the increase in the ambient heat. Furthermore, because the heat transfer process is a process in which the arc gradually cools down, the arc temperature is greater than the ambient temperature [17]. The heat balance equation is as follows:

$$\rho c V \frac{\mathrm{d}T}{\mathrm{d}t} = -hA(T - T_\infty) \quad (1)$$

ρ, c, v, respectively, are arc density, specific heat, and volume; h is the heat transfer coefficient, and A is the arc heat transfer surface area. The excess temperature is $\theta = T - T_\infty$, and the initial conditions of the differential equation are obtained:

$$\theta(0) = T_0 - T_\infty = \theta_0 \quad (2)$$

Separatethe variables for Formula (1), and solve to obtain:

$$\frac{\theta}{\theta_0} = \frac{TT_\infty}{T_0 - T_\infty} = exp(-\frac{hA}{\rho c V} t) \quad (3)$$

The time constant $\tau = \rho c V / h A$ reflecting the heat transfer characteristics is the reciprocal of the exponential part. The characteristic length $l_c = V/A$ of the heat source object represents the equivalent heat conduction distance inside the arc. The conduction thermal resistance of the arc plasma is $R_\lambda = l_c/(\lambda \cdot A)$, and the convective thermal resistance is $R_h = 1/(h \cdot A)$. λ is the thermal conductivity. Biot number indicates the ratio of R_λ to R_h:

$$B_i = \frac{R_\lambda}{R_h} = \frac{hl_c}{\lambda} \tag{4}$$

Assumingthat the arc is a cylindrical heat source with a radius of 5 mm and a height of 3 cm, thermal conductivity $\lambda = 50$ W/(m·K), heat transfer coefficient $h = 18.6$ W/(m^2·K), and specific heat capacity $c = 1.3$ kJ/(kg·K), the characteristic length of the arc l_c is calculated, and Biot number B_i is obtained:

$$B_i = \frac{hl_c}{\lambda} = 0.00225 << 0.1 \tag{5}$$

The results prove that it is feasible to analyze the heat transfer effect in the arc-extinguishing pipe by using the Lumped method, and the time constant of the arc heat transfer system is calculated as follows:

$$\tau = \frac{\rho c V}{hA} = \frac{\rho c l_c}{h} = \frac{0.14 \text{ kg/m}^3 \times 1.3 \text{ kJ}/(\text{kg} \cdot \text{K}) \times 0.0025 \text{ m}}{16.8 \text{ W}/(\text{m}^2 \cdot \text{K})} = 27.1 \text{ µs} \tag{6}$$

Assuming that the initial temperature in the tube is $T_0 = 300$ K, the arc with a critical temperature value of $T_\infty = 3000$ K enters the tube at this time. When air is heated from the initial temperature to $T = 1500$ K during a period, it is substituted into the Formula (3):

$$\frac{\theta}{\theta_0} = \frac{T - T_\infty}{T_0 - T_\infty} = \frac{1500 - 3000}{300 - 3000} = exp(-\frac{t}{\tau}) \tag{7}$$

According to this formula, the transient heat transfer process lasts about 15.9 µs, indicating that the air is heated to a high temperature within a time less than the half-peak value of 8/20 µs impulse lightning current. The arc in the tube can quickly conduct a heat transfer process with the air medium, and the tube air expands when heated. However, due to the structural constraints of the tube, colossal pressure is generated to form a high-temperature airflow. The ideal gas equation can be used to estimate the pressure of a gas heated to 1500 K:

$$P_1 = \frac{T_1}{T_0} P_0 \tag{8}$$

After the gas in the arc-extinguishing pipe is heated and expanded, the pressure is A, and the air pressure rises to five times the original. In the SMTS, the arc heats the air to a high temperature within 27.1 µs, and high-speed airflow is generated in the fractures of each pipe to drive the arc to spray out at the multi-pipe fractures. While accelerating the cooling of the arc, an arc energy breakpoint is formed, which plays the role of blocking the arc. The energy in the arc is reduced, the degree of ionization is reduced until it is extinguished, and the key to arc extinguishing is that the high-speed airflow suppresses the energy of the power frequency arc.

3. Multiphysics Simulation of the Arc-Quenching Process

This paper uses a magnetohydrodynamic (MHD) model for SMTS. In order to describe the arc plasma discharge process, the following assumptions are made [18,19]:

1. Assume that the plasma satisfies local thermodynamic equilibrium. Its physical parameters (conductivity, viscosity coefficient, density, specific heat) are functions of temperature;
2. The arc plasma is set to be compressible laminar flow;
3. The influence of Lorentz force on the fluid is considered.

Arc discharge is a process of multi-physics coupling [20], which leads to the interaction between different physical field parameters, as shown in Figure 2.

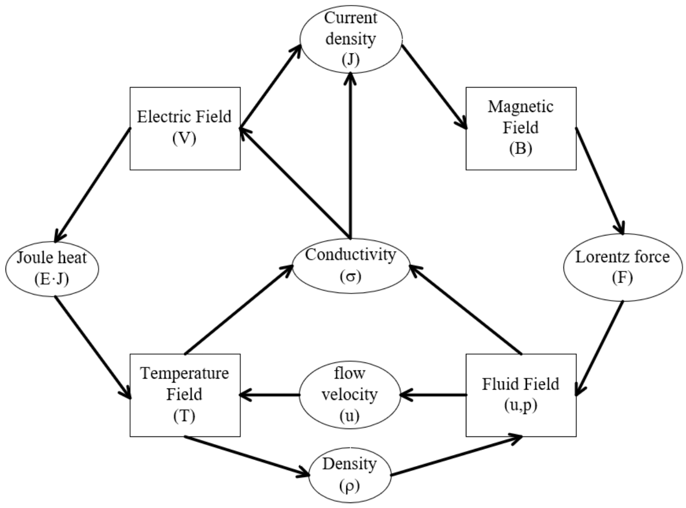

Figure 2. Arc discharge multi-physics field coupling relationship.

The process satisfies the Navier-Stokes equation and the Maxwell equation group, and the continuity equation is as follows:

$$\frac{\partial \rho}{\partial t} + \nabla \cdot (\rho v) = 0 \tag{9}$$

where ρ is the fluid density; v is the velocity vector; and t is the time.

Energy conservation equation:

$$\rho C_P \frac{\partial T}{\partial t} + \rho C_P v \cdot \nabla T - \nabla \cdot (k \nabla T) = \frac{\partial}{\partial T}(\frac{5 k_B T}{2q})(\nabla T \cdot J) + E \cdot J + Q_r \tag{10}$$

C_P is the heat capacity at constant pressure; T is temperature; k is thermal conductivity; Q is the plasma heat source; k_b is the Boltzmann constant; q is the charge per unit electron; E is electric field strength; J is current density; Q_r is radiation heat dissipation quantity.

Momentum conservation equation:

$$\rho(\frac{\partial v}{\partial t} + v \cdot \nabla v) = \nabla \cdot [-pI + \mu(\nabla v + (\nabla v)^T - \frac{2}{3}\mu(\nabla \cdot v)I)] + F \tag{11}$$

where p is the pressure; I is the identity matrix; μ is the dynamic viscosity; B is the magnetic flux density; $F = J \times B$ is the Lorentz force.

Magnetic Field Equations and Current Conservation Equations:

$$\begin{cases} \nabla \times H = J \\ B = \nabla \times A \\ E = -\dfrac{\partial A}{\partial t} \end{cases}, \begin{cases} \nabla \cdot J = Q_{j \cdot V} \\ J = \sigma E + \dfrac{\partial D}{\partial t} + J_e \\ E = -\nabla V \end{cases} \tag{12}$$

H is the magnetic field strength, A is the magnetic vector potential, $Q_{j \cdot V}$ is the charge change per unit volume rate, D is the electric displacement, and V is the electric potential.

3.1. *Simulation Analysis on the Effect of Semi-Closed Tube*

The SMTS is improved from the original multi-compression structure, as shown in Figure 3a,b. The impact of adding a semi-closed structure on lightning discharge is analyzed by comparing the discharge time before and after the improvement. Figure 4a,b show the 2D axisymmetric model with and without the semi-closed tube. In Figure 4a,b, 1 is air, 2 is a metal electrode, and 3 is an insulating material. The simulation model sets five observation points, from coordinates 0.1 cm to 0.9 cm, simulates the potential change of each point, and compares the two structures' discharge times.

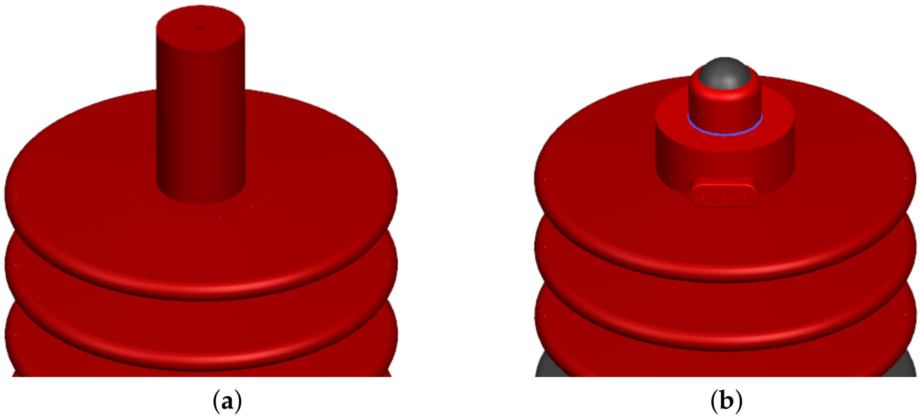

Figure 3. Structural comparison diagram of SMTS and the original multi-compression structure: (**a**) The appearance of SMTS. (**b**) Structure diagram of the original multi-compression structure.

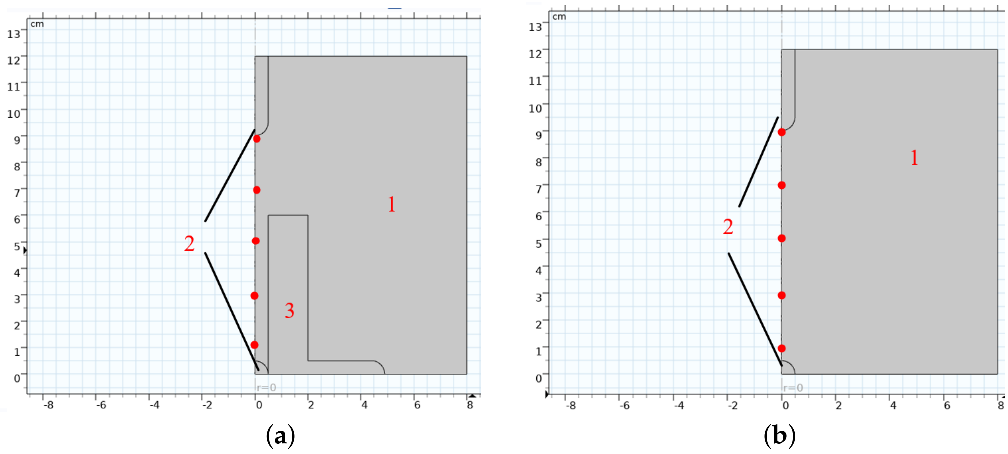

Figure 4. Geometric modeling of SMTS and the original multi-compression structure: (**a**) Model diagram of SMTS. (**b**) Model diagram of the original multi-compression structure.

The lightning current impulse waveform is 8/20 µs waveform, the amplitude is 20 kA, and the simulation results are shown in Figure 5a,b.

Figure 5a is the potential change diagram of each observation point in the SMTS. The results show that the air gap breaks down at 0.15 µs. Figure 5b is the potential change diagram of each observation point in the original multi-compression structure, indicating that the breakdown process is similar to the lightning discharge process, and the lightning discharge begins near the negative electrode until the air gap breaks down at 3.5 µs. The results show that the air gap can be broken down in advance after adding the semi-closed tube, and the initial breakdown time under the impact current can be shortened.

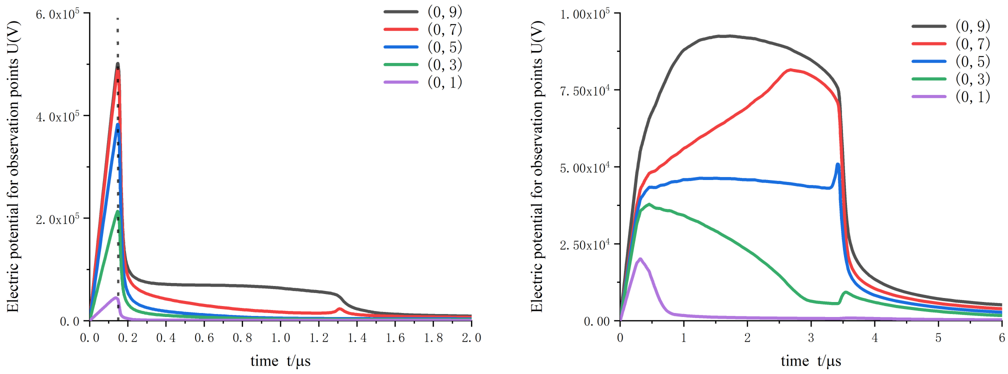

(**a**) (**b**)

Figure 5. Electric potential change curve with time of each observation point: (**a**) Electric potential change curve in SMTS. (**b**) Electric potential change curve in the original multi-compression structure.

3.2. Simulation Analysis of SMTS Arc-Extinguishing Performance

Since the arc path is constrained in multiple tubes during the arc development process, and the arc develops along the axial direction of the compressed pipe, a 2D model can be used for simulation analysis. Figure 6 shows the Comsol 2D model. Added materials include external air medium, metal electrodes, and insulating materials. Numbers 1–6 in the figure are the upper electrode, air, semi-closed tube, copper electrode, shed, and ground electrode, respectively. The air medium is set as compressible laminar flow, the initial temperature is 298 K, and the initial pressure is 1.01×10^5 Pa; a 20 kA 8/20 μs impulse current is applied to the upper electrode, and a power frequency current with an amplitude of 1.5 kA is coupled. Set the lower electrode as the ground electrode, and select the simulation time step to be 1 μs and the simulation time to be 2 ms. A to E are the five observation points close to the nozzle set by the simulation model to measure the change in temperature and conductivity with time.

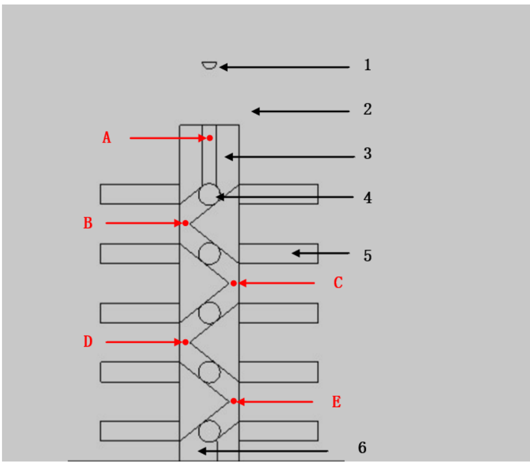

Figure 6. Simulation model diagram.

The simulation focuses on developing high-temperature airflow in the multi-channel structure. It simulates the lightning impulse waveform to cause the air discharge in the structure to form an arc channel. According to the energy balance theory, the convective heat transfer between the air medium in the tube and the arc is a balanced process. The lightning pulse is measured in instantaneous Joule. The heat source input is much greater than the energy dissipation at this time, the temperature in the SMTS rises sharply, and thermal breakdown is formed along the arc channel formed by the electrodes.

Figure 7 is a temperature distribution diagram of the SMTS. At 10 μs, the temperature around the upper electrode and the ground electrode gap increased first. Then the temperature of all inner gaps and the air gap between electrodes increased, but no high-temperature channel gap was formed without breakdown. At 50 µs, the high-temperature arc channel was formed due to the breakdown discharge in the inter-structure gap due to the lightning impulse. At 200 µs, the maximum temperature inside the SMTS is about 11,000 K. After 200 µs, the arc is affected by the high-temperature gas flow ejected from the axial semi-closed tube and the multi-compression tubes, and the temperature begins to drop. At 1000 µs, the temperature in the entire channel drops below 3000 K, which is 3000 K lower than the critical temperature of the arc, and it can be considered that the arc has lost its conductivity.

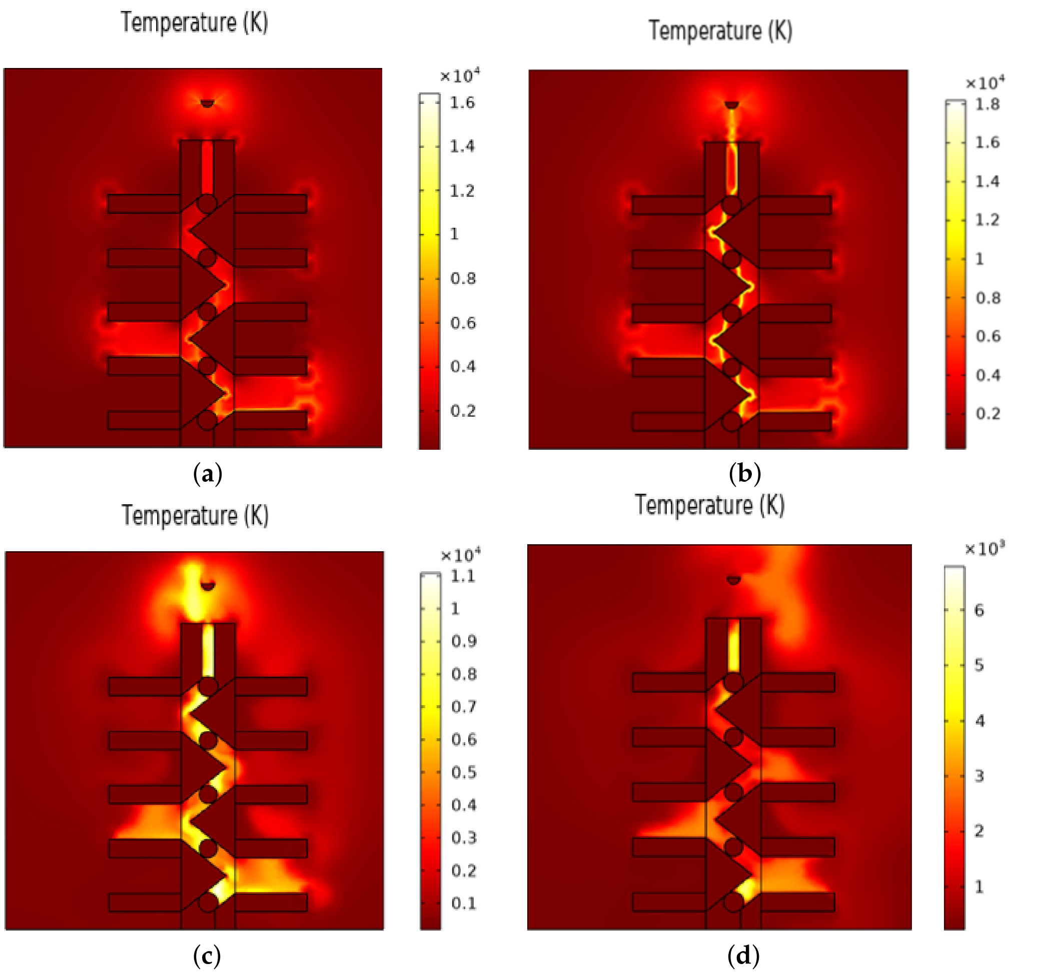

Figure 7. Arc temperature change diagram in the simulation area at different moments: (**a**) t = 10 µs; (**b**) t = 50 µs; (**c**) t = 200 µs; (**d**) t = 1000 µs .

Conductivity is a physical quantity that reflects the conductivity of the medium. It can determine whether the arc-extinguishing channel is in a medium state. The dissociation of the air medium increases as temperature increases, and air changes from an insulator to a conductor.

Figure 8 is a cloud diagram of the SMTS conductivity distribution. At 10 µs, the model starts to arc and has not yet developed into a complete breakdown channel. At 50 µs, a conductive channel through the electrode appears, and conductivity reaches a maximum of 296 S/m, similar to the temperature change. At 200 µs, the long arc is affected by the high-speed airflow and is divided into several short arcs. After the arc is cut off, the source of lightning energy is lost, the temperature begins to drop, the conductivity drops sharply, and the high conductivity area gradually presents a truncated distribution. At 1000 µs, the conductivity of most areas drops to zero, and the arc-extinguishing channel completely recovers its insulation.

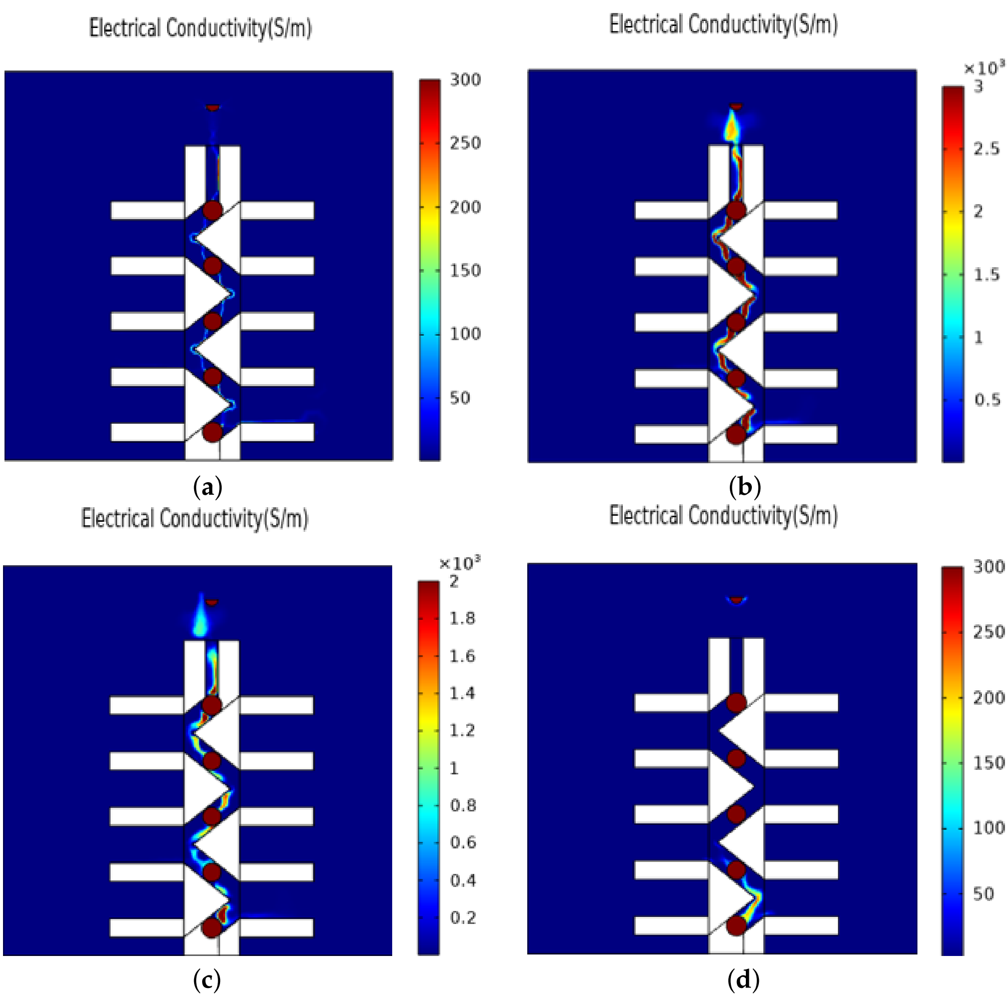

Figure 8. Arc conductivity change diagram in the simulation area at different moments: (**a**) t = 10 µs; (**b**) t = 50 µs; (**c**) t = 200 µs; (**d**) t = 1000 µs.

Figure 9a is the temperature change curve of each observation point. The temperature change has the characteristics of a rapid rise and slow fall. It rises rapidly in the early stage of arc development and reaches a peak of 11,000 K at 200 µs. After that, the temperature begins to fall and returns to a lower value after about 2 ms.

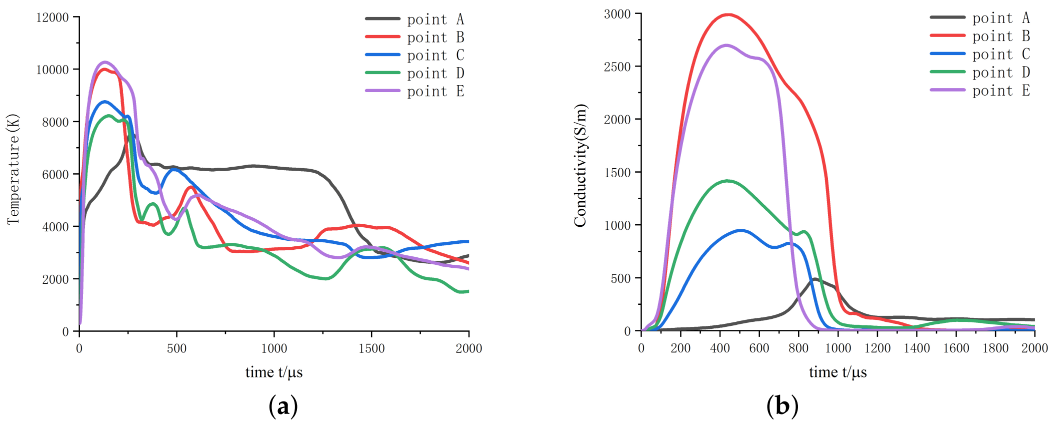

Figure 9. Observation point temperature and conductivity change curve: (**a**) Observation point temperature change curve. (**b**) Observation point temperature change curve.

Figure 9b is the conductivity change curve of each observation point. The conductivity at the observation point has the characteristics of uneven distribution; at the observation point of the multi-tubes it reaches a peak value at 500 μs, and 900 μs at the observation point of the semi-closed tube. At 1 ms, the multi-tubes are basically restored to the initial value, and it can be considered that the arc has been extinguished.

4. Analysis of Test Results

4.1. Test Preparation

This paper used a shock and power frequency joint arc-extinguishing test platform to verify the simulation analysis results. The test circuit is shown in Figure 10, mainly including the impulse voltage trigger circuit and the power frequency freewheeling trigger circuit. T is a power frequency test generator; R is an overcurrent protector; C1, C2, C3, and C4 are capacitors; MOA1 and MOA2 are metal oxide arresters; L is an inductor; S1 and S are the breakdown ball gap; S2 is the protection ball gap; TO is the semi-closed multi-compression tube arc-extinguishing structure test sample; TA is the Rogowski coil; Rf is the wave head resistance; Rt is the wave tail resistance; C5 is the capacitor; DIVMS is a digital oscilloscope; and IG is a lightning impulse voltage generator.

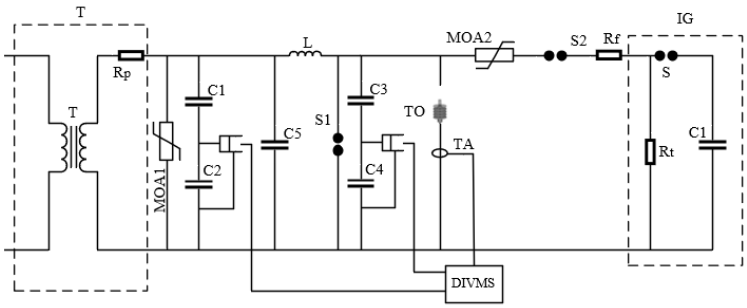

Figure 10. Combined test circuit diagram of high impulse current and power frequency freewheeling.

The test process is as follows:

1. Before applying the impulse voltage, start the power frequency power supply and maintain it for a while;
2. First, without installing the SMTS, start the impulse voltage generator, break down the air gap, and measure the impulse current waveform;
3. Build the test circuit, check the test product and install the test product in the circuit, ground the circuit effectively, adjust the shooting angle of the high-speed camera, install and debug DIVMS, and record the test waveform and arc-extinguishing process;
4. Start the impulse voltage generator. After charging is completed, control the trigger circuit to discharge the test product and measure the impulse current waveform and power frequency current waveform of the arc-extinguishing structure installed.

4.2. Analysis of Test Results

A high-speed camera is used to photograph the power frequency freewheeling interruption process of the SMTS. The arc-extinguishing process is shown in Figure 11: Figure 11a shows that the SMTS is instantaneously broken down, and after the arc enters the channel, it is coupled with the air in the arc-extinguishing structure. Figure 11b illustrates that the airflow in the pipeline expands and heats up rapidly under the action of arc heating in the pipeline, forming a high-temperature and high-speed airflow. Under high-speed airflow, the arc is ejected along the axial semi-closed tube and the nozzle of the axial multi-compression tube. Figure 11c shows no residual arc between the fractures, indicating that the arc has been further weakened at this time, and the arc channel is closed, preventing the power frequency energy from continuously entering the SMTS. Figure 11d shows that the arc cannot maintain its combustion, and the high-speed airflow accelerates the process of cooling and deionization. Figure 11e,f show that the arc has been substantially extinguished, and no reignition has occurred.

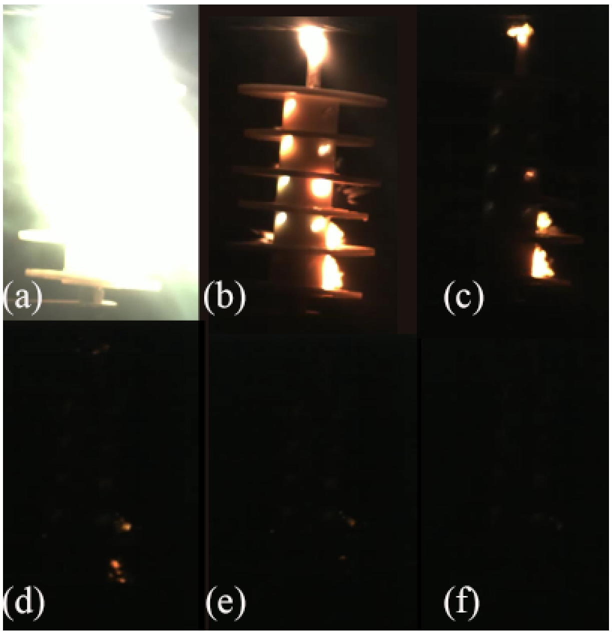

Figure 11. Arc-extinguishing process captured by high-speed camera.

Figure 12 is the power frequency current arc-extinguishing waveform, CH1 represents the voltage waveform channel, and CH2 represents the current waveform channel. The SMTS is broken down under the action of impulse voltage. Due to the arc extinguishing effect of the SMTS, the voltage waveform fluctuated slightly but quickly recovered to the rated value within one cycle, and the frequency was maintained at 50 Hz. At this time, the peak value of the power frequency current was measured to be 0.673 kA, and due to the suppression of the high-speed airflow, the current value dropped rapidly. After the current impulse discharge is over, due to the weakening of the airflow, the suppression effect of the airflow on the power frequency arc is also weakened, the descending speed of the arc current slows down, and the inflection point of the arc current decline appears at the end of the lightning. The measured current dropped to 0 in 1 ms, indicating that the power frequency freewheeling was successfully blocked and the reignition was suppressed.

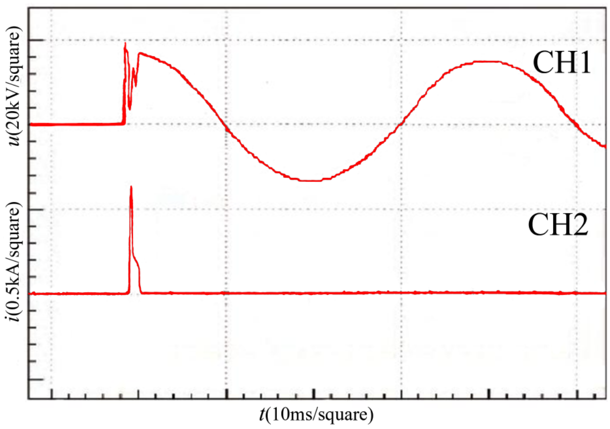

Figure 12. Combined test of high impulse current and power frequency freewheeling test voltage waveform (CH1) and current waveform (CH2).

5. Conclusions

This paper describes the arc-extinguishing simulation and experiment of the semi-closed multi-compression tube structure.

(1) The results of the simulation comparison experiment with or without a semi-closed tube show that the improved SMTS adds a semi-closed tube, which can shorten the breakdown time of the impulse voltage;
(2) The simulation and test have mutually confirmed the suppression effect of the SMTS on the arc. The lightning energy accumulates in the SMTS to form a high-speed airflow, which accelerates the dissipation of the arc energy. In addition, it is also determined that the arc-extinguishing time of the SMTS is about 1 ms. According to the test, the SMTS can interrupt the power frequency freewheeling arc with a peak value of 0.673 kA.

Author Contributions: Conceptualization, J.W.; Data curation: Y.S.; Formal analysis, Y.L. and H.L.; Investigation: Y.S. and Z.J.; Methodology: Y.S., J.W. and Q.H.; Project administration: Y.W. and P.H.; Resources: J.W.; Software, Y.S.; Supervision: J.W.; Validation: Z.J.; Writing—original draft: Y.S.; Writing—review and editing: Y.S. All authors have read and agreed to the published version of the manuscript.

Funding: This research was funded by the Guangxi innovation driven development project of the Guangxi Science and Technology Department grant number AA18242050.

Data Availability Statement: Not applicable.

Conflicts of Interest: The authors declare no conflict of interest.

Abbreviations

The following abbreviations are used in this manuscript:

SMTS	Semi-Closed Multi-Compression Tube Structures

References

1. Chen, Y.; Wang, J.; Huang, P.; Wang, Y.; Zhang, Y. Arc-extinguishing characteristics of semi-enclosed structures based on theory of positive shock wave reflection. *AIP Adv.* **2022**, 12, 015009. [CrossRef]
2. Li, C.; Su, K.; Zhang, Y.; Lu, Z. Backflash Simulation Research on Substation Ground Potential Rise to Low Voltage Arrester. *Insul. Surge Arresters* **2020**, *4*, 178–183. [CrossRef]
3. Masłowski, G.; Hajder, S. Measurements and Modeling of Long Continuing Current in the Lightning Protection System of a Residential Building. *Energies* **2022**, *15*, 6862. [CrossRef]
4. Xie, C.; Bai, J.; Wang, H. Lightning risk assessment of transmission lines based on multidimensional related information fusion. *Proc. CSEE* **2018**, *38*, 6233–6244+6485. [CrossRef]
5. Ohtaka, T.; Kameda, H. Effective Installation Strategies of Fault Current Interrupting Arcing Horns Considering Operational Coordination with Responses of Line Protection Relays. *Electr. Eng. Jpn.* **2018**, *202*, 3–11. [CrossRef]
6. Jia, W.; Sima, W.; Yuan, T. 3D simulation and experiment research on arc motion characteristics in the semi-enclosed arc-extinguishing chamber. *Trans. China Electrotech. Soc.* **2021**, *36*, 321–329. [CrossRef]
7. Lu, G.; Luo, J.; Liu, H. Statistics and simulationof lightning trip out of transmission linesin Guangzhou area. *High Volt. Eng.* **2018**, *44*, 1542–1548. [CrossRef]
8. Li, Q.; Wang, J.; Hang, Y. Study on performance of air-blowing arc-quenching device based on the mhd theory. *Power Syst. Technol.* **2020**, *46*, 2025–2031.
9. Yang, X.; Zhu, H.; Zhong, M. Single-phase installation method of parallel gap in 10kv distribution line. *Power Syst. Technol.* **2020**, *44*, 3164–3171. [CrossRef]
10. Wang, Y.; Luo, Y.; Chen, Y.; Wang, J. Electric Arc Recoil—A Novel Method for Reducing Lightning Strike Potential Difference for Transmission Line. *IEEE Access* **2021**, *9*, 79663–79670. [CrossRef]
11. Bi, J.; Wang, J.; Wang, X. Simulation and experimental study on multiple lightning protection process under principle of solid phase arc extinguishing device. *High Volt. Appar.* **2022**, *58*, 108–114+123. [CrossRef]
12. Markhotok, A. The effect of gas nonideality on the interface reflectivity when interacting with a shock wave. *IEEE Trans. Plasma Sci.* **2020**, *48*, 3759–3767. [CrossRef]
13. Li, Z.; Wang, J.; Zhou, X.; Huang, S.; Xia, Z. DC arc suppression in the improved multi-chamber structure. *AIP Adv.* **2019**, *9*, 055115. [CrossRef]
14. Li, Z.; Wang, J.; Zhou, X. Study on impulse quenching based multi-chamber arc quenching structure. *AIP Adv.* **2019**, *9*, 085104. [CrossRef]
15. Bityurin, V.A.; Bocharov, A.N. MHD heat flux mitigation in hypersonic flow around a blunt body with ablating surface. *J. Phys. D Appl. Phys.* **2018**, *51*, 264001. [CrossRef]

16. Bocharov, A.N.; Mareev, E.A.; Popov, N.A. Numerical simulation of high-current pulsed arc discharge in air. *J. Phys. D Appl. Phys.* **2022**, *55*, 115204. [CrossRef]
17. Xia, Y.; Wu, X. Study on Conductivity Calculation of Local Thermodynamic Equilibrium Arc Plasma. *Electr. Switch* **2020**, *58*, 19–23.
18. Shen, H.; Lei, T.; He, Z. Parameter Selection Suggestion of Power Frequency Follow Current Interruption Capability for Multi-chamber Gap Lightning Protection Device Used in 10 kV Distribution Lines. *Power Syst. Technol.* **2019**, *43*, 1480–1486. [CrossRef]
19. Schlitz Lei, Z.; Garimella Suresh, V.; Chan, S.H. Gas dynamics and electromagnetic processes in high-current arc plasmas. Part I. Model formulation and steady-state solutions. *J. Appl. Phys.* **1999**, *85*, 2540–2546. [CrossRef]
20. Wu, S.; Xiong, L.; Yang, Z.; Chen, Y.; Zhang, Z. Simulation and experimental study on electrode erosion characteristics of wire by DC arc. *High Volt. Eng.* **2022**, *48*, 3316–3325. [CrossRef]